J Therm Anal Calorim (2017) 127:1511–1521
DOI 10.1007/s10973-016-5573-9

Spectral, magnetic, thermal and biological studies on Ca(II) and Cu(II) complexes with a novel crowned Schiff base

Irina Zarafu[1] · Mihaela Badea[2] · Gabriela Ioniţă[3] · Petre Ioniţă[1] · Anca Păun[1] · Marcela Bucur[4,5] · Mariana Carmen Chifiriuc[4,5] · Coralia Bleotu[6] · Rodica Olar[2]

Received: 19 January 2016 / Accepted: 14 May 2016 / Published online: 18 June 2016

Abstract A series of complexes $[Ca(HL)(OH_2)_4]Cl_2 \cdot 4H_2O$ (**1**), $[CuL_2] \cdot 2H_2O$ (**2**) and $[Cu\{Ca(L)(OH_2)_2\}_2]Cl_4 \cdot H_2O$ (**3**) (HL: 2-hydroxy-8-methyl-tricyclo[7.3.1.$0^{2,7}$]tridec-13-N-4′(benzo-15-crown-5-ether)-imine) were synthesised and characterised. The features of complexes have been assigned from microanalytical data, IR, UV–Vis–NIR and EPR spectra, magnetic data at room temperature as well as thermal analysis. The ligand coordinates through azomethinic nitrogen and hydroxylic oxygen at Cu(II) and through etheric oxygen at Ca(II). The electronic and EPR spectra suggest a square planar stereochemistry for Cu(II). The thermal analysis evidenced that thermal transformations are complex processes according to DTG and DTA curves including (crystallisation or coordination) water elimination, thermolyses and oxidative degradation of Schiff base. The results of the biological assays revealed that the complexes exhibited good antimicrobial activity against planktonic and sessile bacterial and fungal strains.

Keywords Complex · Crowned Schiff base · Thermal behaviour · Antimicrobial · Antibiofilm · Cytotoxicity · Antioxidant

Introduction

During the past decades, considerable attention has been paid to the chemistry of complexes with Schiff bases containing supplementary groups that allow these species to perform different functions or induce them useful properties [1]. On the other hand, the rapid development of the field of hetero-binucleating ligands as well as the coordination chemistry provided by them has prompted an extension of studies on the synthesis of functionalised Schiff base. Among them, the crown ether-containing Schiff bases have attracted much attention because the crown moiety could endow functional molecules with novel performance and character owing to the hydrophobicity of the outer ethylene groups and orderly arrangement of inner oxygen atoms [2–7].

So far benzocrown ether derivatives were grafted into bidentate NO [2, 3], NS [4], three-dentate N_2O [5], four-dentate N_2O_2 [6] or bis(dicompartimental) four-dentate N_2O_2 [7] Schiff base ligands. Such derivatives can be synthesised by one step procedure involving the condensation reaction between an amine derivative and a carbonyl species, one of them bearing the crown ether moiety [2–7].

Electronic supplementary material The online version of this article (doi:10.1007/s10973-016-5573-9) contains supplementary material, which is available to authorized users.

✉ Rodica Olar
rodica.olar@chimie.unibuc.ro

[1] Department of Organic Chemistry, Faculty of Chemistry, University of Bucharest, 90-92 Panduri Str., Sector 5, 050663 Bucharest, Romania

[2] Department of Inorganic Chemistry, Faculty of Chemistry, University of Bucharest, 90-92 Panduri Str., Sector 5, 050663 Bucharest, Romania

[3] Romanian Academy, "Ilie Murgulescu" Physical Chemistry Institute, 202 Splaiul Independentei, 060021 Bucharest, Romania

[4] Department of Microbiology, Faculty of Biology, University of Bucharest, 1-3 Aleea Portocalilor St., 60101 Bucharest, Romania

[5] Research Institute of the University of Bucharest, Spl. Independentei 91-95, Bucharest, Romania

[6] Stefan S Nicolau Institute of Virology, 285 Mihai Bravu Ave., Bucharest, Romania

It is known that the azomethine moiety generates stable complexes with most metal ions and especially with transition ones [1], but the crown ether units have a large affinity for main groups and lanthanides metal ions [4, 5, 8–11]. As result, the redox and electronic properties of the transition metal centre can be modulated through the size and charge of the hard metal ions bound to the crown ether moiety. On the other hand, such complexes can be used as sensors for ammonium or diammonium cations [12, 13] as well as alkaline, alkaline earth and lanthanide metal ions both in solution [2, 7, 14] and deposited in polymeric films [15].

The crown ethers have selectivity for a particular metal ion according to their particular molecular structure. In order to improve this selectivity for metal ions and find applications in hard metal extraction from different sources, some crown ethers were crosslinked to chitosan [16, 17].

Having in view their host–guest recognition properties, the crown ether complexes may provide useful models for hydrolases as result of the fact that the crown rings can offer a hydrophobic environment provided by the outer ethylene groups. The studies showed that some crowned Schiff base complexes containing transition metal ions exhibit a high activity in the catalytic hydrolysis of phosphate [18, 19] or picolinate esters, respectively [20], in micellar solution.

In the last years, a number of reports concerning the Schiff base complexes containing crown ether rings ability to bind O_2 and thus perform catalytic oxidation of various organic compounds [21–26] were published. It was observed that the complexation of a hard cation in the crown ether cavity of these catalysts, close to the transition metal centre, perturbs the oxygen-binding properties of the metal centre which results in an improved catalytic behaviour of some catalysts in comparison with their acyclic analogues [21]. Cobalt(II) complexes with some crowned Schiff base were studied either as metallomicelles and or as peroxidase mimics [27]. Sodium complexes with the bis-crown ether-derived Schiff bases have been shown to exhibit antibacterial activity against *Staphylococcus epidermidis* [11].

So far there is no report concerning thermal behaviour of this type of Schiff base or their complexes. As result, in the present work, this field was extended in the synthesis of complexes with the novel crowned Schiff base (2-hydroxy-8-methyl-tricyclo[7.3.1.$0^{2.7}$]tridec-13-N-4′(benzo-15-crown-5-ether)-imine). In order to explore both coordinative sites, crown ether cavity and the NO donor atoms set, respectively, new complexes with Ca(II), Cu(II) and both Ca(II) and Cu(II) were synthesised and characterised. The details of synthesis, spectral, magnetic and thermal behaviour of these compounds are described in the following. Ligand and complexes were screened for their antioxidant, antimicrobial and cytotoxic behaviour.

Experimental

Materials

Starting materials (chemicals, TLC plates, $CaCl_2$, $CuCl_2$·$2H_2O$) and solvents were purchased from Sigma-Aldrich and Chimopar and used as received.

Instruments

Carbon, hydrogen and nitrogen contents were determined with a PerkinElmer PE 2400 analyser. The metal ion content was determined volumetrically by using complexometric or iodometric method, respectively [28]. Each sample was treated with few drops of concentrated H_2SO_4 and hydrogen peroxide and heated to dry. The residue was redissolved in distilled water, the pH was adjusted with ammonia–ammonium chloride buffer, and the calcium content was determined by titration with 0.1 M solution of $Na_2MgEDTA$ by using Eriochrome Black T as indicator. The copper-containing samples were treated with KI and KSCN in acidic medium, and the released iodine was titred with 0.1 M solution of sodium thiosulphate in the presence of amidon.

The molar conductance was determined for 10^{-3} M solutions of complexes in DMSO with a multi-parameter analyser Consort C861.

Mass spectra were recorded with API 6500 AB SCIEX, Canada, mass spectrometer with ESI source (Turbo spray model AB SCIEX) operating in positive mode. Samples were dissolved in DMF at 1 mg mL^{-1}, and then the solution was diluted with methanol up to a final concentration of 1 μg mL^{-1}. Molecular ions scanning range (*m/z*) was 0–1250.

IR spectra were recorded in KBr pellets with a Bruker Tensor 37 spectrometer in the range 400–4000 cm^{-1}.

Electronic spectra by diffuse reflectance technique, with spectralon as standard, were recorded in the range 200–2000 nm, on a Jasco V-670 spectrophotometer.

^{1}H-NMR and ^{13}C-NMR spectra were recorded on a Varian Inova-400 spectrometer at selected temperatures, in deuterated solvents $CDCl_3$ and DMSO-d_6, isotopic purity 99.9 % (the atoms notation in NMR spectra is presented in Supplementary material).

The melting point was determined with a Böetius apparatus and Krous device.

Magnetic measurements were taken at room temperature, on a Lake Shore's fully integrated Vibrating Sample Magnetometer (VSM) system 7404, calibrated with a Ni—0.126 g sphere—SRM 772a. The VSM was intercalibrated either with an absolute calibrated Faraday balance or with $Hg[Co(NCS)_4]$ as standard. The molar magnetic

susceptibilities were calculated and corrected for the atomic diamagnetism.

The X-band EPR measurements were taken at 293 K for solid sample and at 100 K for DMSO solution on a JEOL FA100 spectrometer. The general settings used were as follows: sweep field 1000 G, frequency 100 kHz, gain in the range 100–200, sweep time 1800 s, time constant 1 s, modulation width 2 G, microwave power 1 mW. The magnetic field calibration was performed with a DPPH (2,2-diphenyl-1-picrylhydrazyl) standard marker, exhibiting a narrow EPR line with g factor 2.0036.

The TG, DTG and DTA curves were recorded using a Labsys 1200 SETARAM instrument, over the temperature range of 20–900 °C with a heating rate of 10 °C min^{-1}. The measurements were taken in synthetic air atmosphere (flow rate 17 cm^3 min^{-1}) by using alumina crucibles.

Antioxidant capacity

The total antioxidant activity (TAC) was evaluated by the DPPH method [29]. A fresh solution of $2{\cdot}10^{-4}$ M DPPH in methanol was prepared and kept in dark till was used, and compounds were also dissolved in methanol at a concentration of 1 mg mL^{-1}. A blank sample was obtained from 1.8 mL solution of DPPH and 0.2 mL of pure methanol, while working samples were obtained from 1.8 mL solution of DPPH and 0.2 mL solution of each compound. After mixing, each sample was kept in the dark for 30 min, followed by absorbance measurement at 517 nm.

The total antioxidant capacity (TAC) was calculated with Eq. 1:

$$\% \text{ Inhibition} = \text{Abs}_{\text{ini}} - \text{Abs}_{30\text{min}}/\text{Abs}_{\text{ini}} \times 100 \quad (1)$$

where Abs_{ini} represents the initial absorption of DPPH radical at 517 nm and $\text{Abs}_{30\text{min}}$ is the absorbance recorded after 30 min at the same wavelength.

Antimicrobial assays

The antimicrobial assays were performed on reference (bearing the ATCC code) microbial strains, i.e., gram-positive (*Staphylococcus aureus* ATCC 6538, *Staphylococcus saprophyticus* ATCC 15305, *Bacillus subtilis* ATCC 6633) and gram-negative (*Escherichia coli* ATCC 8739, *Pseudomonas aeruginosa* ATCC 27853) bacteria, as well as the fungal strain *Candida albicans* ATCC 26790. The qualitative evaluation of the antimicrobial activity was performed by the adapted disk diffusion, as previously reported [30], using Mueller–Hinton Agar (MHA) medium for bacteria and Yeast Peptone Glucose (YPG) in case of fungi. The compounds were solubilised in dimethylsulphoxide (DMSO), and the starting stock solution was of 1000 μg mL^{-1} concentration.

The quantitative assay of the antimicrobial activity was performed by the liquid medium microdilution method, in 96 multi-well plates, in order to establish the minimal inhibitory concentration (MIC) and the minimal biofilm eradication concentration (MBEC) values [30]. All biological experiments were performed in triplicates.

Cytotoxicity assay

The compounds cytotoxicity was evaluated on human tumour cell line HCT 8 (human ileocecal adenocarcinoma). HCT 8 cells ($5{\cdot}10^5$) were seeded in 3.5-cm-diameter Petri dish and treated with 250 μg mL^{-1} compounds for 24 h. The cells were resuspended in 100 μL of binding buffer (10 mM of HEPES/NaOH, pH value 7.4, 140 mM NaCl and 2.5 mM $CaCl_2$), and stained with 5 μL Annexin V-FITC and 5 μL propidium iodide for 10 min in dark. At least 10,000 events from each sample were acquired using a Beckman Coulter flow cytometer. The percentage of treatment affected cells was determined by subtracting the percentage of apoptotic/necrotic cells in the untreated population from percentage of apoptotic cells in the treated population.

Synthesis and analytical data for 2-hydroxy-8-methyl-tricyclo[7.3.1.$0^{2,7}$]tridec-13-N-4′(benzo-15-crown-5)-imine (HL) and complexes

For HL to 1 mmol of 2-hydroxy-8-methyl-tricyclo[7,3,1,02,7]-13-one-tridecane dissolved in 8 mL ethanol was added 1 mmol of 4′-aminobenzo-15-crown-5-ether. The mixture was stirred and refluxed for 30 min and afterword was stirred at room temperature overnight. The reaction was stopped, and the solvent was removed under reduced pressure. A solid was formed with 93 % yield. The purity of the obtained product was checked with thin layer chromatography using CH_2Cl_2: MeOH (5:0.5, *v/v*) as eluent. The β-cycloketol derivative was obtained by a Michael reaction by using a modified Tilicenko-Barbulescu method [31, 32]. Yield 93 %. Analysis found: C, 68.91, H, 8.44, N, 2.83, $C_{28}H_{41}NO_6$ calculate: C, 68.97, H, 8.48, N, 2.87 %; m. p. 72–73 °C; ESI–MS (positive mode, CH_3CN:CH_3OH) *m/z*: $[M\text{-}3H]^+$, 484.2; $[C_{27}H_{34}NO_6]^+$, 468.4; $[C_{25}H_{32}NO_6]^+$, 442.1; $[C_{24}H_{30}NO_6]^+$, 428.1; $[C_{18}H_{34}NO_5]^+$, 344.3; $[C_{15}H_{27}NO_5]^+$, 301.4; $[C_{15}H_{28}NO]^+$, 226.3; $[C_{11}H_{16}O]^+$, 164.0; $[C_7H_8N]^+$, 106.6; $[C_6H_{11}]^+$, 83.4; $[C_6H_{11}]^+$, 83.4; ^{1}H-NMR (400 MHz, $CDCl_3$, 303 K, δ (ppm), *J* (Hz)): 6.72 (d, 1H, H-5, 8.4); 6.27 (d, 1H, H-2, 2.5); 6.20 (dd, 1H, H-6, 2.5, 8.4); 4.02–4.10 (m, 4H, H-20, H-27, syst. A_2B_2); 3.84–3.92 (m, 4H, H-21, H-26, syst. A_2B_2); 3.75 (s, 8H, H-22 ÷ H-25); 3.50 (bs, 1H, OH); 2.29 ÷ 2.17 (m, 4H, H-8, H-9, H-10, H-12); 2.11 ÷ 1.57 (m, 4H, H-aliph.); 1.52 ÷ 1.20 (m, 10H, H-aliph.); 1.02

(d, 3H, H-9′, 7.0); ^{13}C-NMR ($CDCl_3$, 303 K, δ ppm): 219.59 (C-7); 150.55 (C-3); 141.95 (C-1); 141.62 (C-4); 117.51 (C-5); 107.29 (C-6); 102.70 (C-2); 78.09 (C-11); 70.99 (CH_2-CE); 70.91 (CH_2-CE); 70.85 (C-23, C-24); 70.54 (CH_2-CE); 69.99 (CH_2-CE); 69.65 (CH_2-CE); 68.74 (CH_2-CE); 59.89 (CH); 52.75 (CH); 45.89 (CH); 37.56 (CH); 36.47 (CH_2); 29.30 (CH_2); 28.88 (CH_2); 26.19 (CH_2); 25.51 (CH_2); 21.24 (CH_2); 20.18 (CH_2); 15.86 (C-9′) (CE, crown ether moiety) (The atom numbering is presented in Figure 1S).

$[CaL(OH_2)_4]Cl_2{\cdot}4H_2O$ (**1**): To a solution containing 0.111 g (1 mmol) calcium(II) chloride in 10 mL water was dropwise added a solution obtained by 0.49 g (1 mmol) (HL) dissolved in 10 mL ethanol. The reaction mixture was refluxed for 4 h until the colour was slightly modified to light brown. The solution was cooled and dried at room temperature. The solid product was resumed with acetone, filtered off, washed with acetone and air-dried. Analysis found: Ca, 5.32; C, 45.34; H, 7.66; N, 1.92, $CaC_{28}H_{57}NO_{14}Cl_2$ calculate: Ca, 5.40; C, 45.28; H, 7.74; N, 1.89 %; Yield 78 %; ^{1}H-NMR (400 MHz, DMDO d_6, 303 K, *δ* (ppm), *J* (Hz)): 6.63 (d, 1H, H-5, 8.2); 6.22 (d, 1H, H-2, 2.4); 6.05 (dd, 1H, H-6, 2.4, 8.2); 4.58–4.80 (m, 4H, H-20, H-27, syst. A_2B_2); 3.85–4.05 (m, 4H, H-21, H-26, syst. A_2B_2); 3.72 (s, 8H, H-22 ÷ H-25); 3.48 (bs, 1H, OH); 1.75–2.16 (m, 4H, H-8, H-9, H-10, H-12); 1.49–1.72 (m, 4H, H-aliph.); 1.20–1.45 (m, 10H, H-aliph.); 0.93 (d, 3H, H-9′, 6.8); ^{13}C-NMR ($CDCl_3$, 303 K, δ ppm): 217.44 (C-7); 149.93 (C-3); 143.97 (C-1); 139.36 (C-4); 117.51 (C-5); 105.57 (C-6); 101.03 (C-2); 76.37 (C-11); 72.32 (CH_2-CE); 70.32 (CH_2-CE); 70.16 (C-23, C-24); 70.07 (CH_2-CE); 69.80 (CH_2-CE); 69.75 (CH_2-CE); 68.85 (CH_2-CE); 60.17 (CH); 52.19 (CH); 45.25 (CH); 36.45 (CH); 35.33 (CH_2); 28.92 (CH_2); 28.92 (CH_2); 28.72 (CH_2); 25.81 (CH_2); 20.80 (CH_2); 19.75 (CH_2); 15.62 (C-9′); ESI–MS (positive mode, DMF:CH_3OH) *m/z*: $[M\text{-}4H_2O\text{–}3H]^+$, 594.7; $[CaC_{27}H_{36}NO_6Cl_2]^+$, 581.7; $[CaC_{28}H_{41}NO_6Cl]^+$, 563.5; $[C_{28}H_{38}NO_6]^+$, 484.2; $[C_{27}H_{34}NO_6]^+$, 468.4; $[C_{25}H_{32}NO_6]^+$, 442.1; $[C_{24}H_{30}NO_6]^+$, 428.1; $[C_{18}H_{34}NO_5]^+$, 344.3; $[C_{15}H_{27}NO_5]^+$, 301.4; $[C_{15}H_{28}NO]^+$, 226.3; $[C_{11}H_{16}O]^+$, 164.0; $[C_7H_8N]^+$, 106.6; $[C_6H_{11}]^+$, 83.4; $[C_6H_{11}]^+$, 83.4; Λ_M, 142 Ω^{-1} cm^2 mol^{-1}.

$[CuL_2]{\cdot}2H_2O$ (**2**): To a solution containing 0.085 g (0.5 mmol) copper(II) chloride dihydrate in 20 mL ethanol was dropwise added a solution obtained by 0.49 (1 mmol) HL dissolved in 10 mL ethanol and few drops of 25 % ammonia solution. The reaction mixture was refluxed for 4 h until a solid product, and brown coloured was obtained. The compound was filtered off, washed with ethanol and air-dried. Analysis found: Cu, 5.86; C, 62.83; H, 7.76; N, 2.62, $CuC_{56}H_{84}N_2O_{14}$ calculate: Cu, 5.92; C, 62.69; H, 7.89; N, 2.61 %; Yield 75 %; ESI–MS (positive mode, DMF:CH_3OH) *m/z*: $[M\text{–}2H_2O\text{–}CH_3\text{–}4H]^+$, 1017.7; $[CuC_{54}H_{73}N_2O_{12}]^+$, 1005.5; $[CuC_{53}H_{70}N_2O_{12}]^+$, 990.5; $[CuC_{47}H_{60}N_2O_{12}]^+$, 908.4; $[CuC_{53}H_{70}N_2O_{12}]^+$, 990.5; $[C_{28}H_{38}NO_6]^+$, 484.2; $[C_{27}H_{34}NO_6]^+$, 468.4; $[C_{25}H_{32}NO_6]^+$, 442.1; $[C_{24}H_{30}NO_6]^+$, 428.1; $[C_{18}H_{34}NO_5]^+$, 344.3; $[C_{15}H_{27}NO_5]^+$, 301.4; $[C_{15}H_{28}NO]^+$, 226.3; $[C_{11}H_{16}O]^+$, 164.0; $[C_7H_8N]^+$, 106.6; $[C_6H_{11}]^+$, 83.4; $[C_6H_{11}]^+$, 83.4; Λ_M, 16 Ω^{-1} cm^2 mol^{-1}.

$[Ca_2CuL_2(OH_2)_4]Cl_4{\cdot}H_2O$ (**3**): To a solution containing 0.111 g (1 mmol) calcium(II) chloride and 0.085 g (0.5 mmol) copper(II) chloride dihydrate in 20 mL water was dropwise added a solution of 0.49 g (1 mmol) HL in 10 mL ethanol and few drops of 25 % ammonia solution. The reaction mixture was refluxed for 6 h until the colour was slightly modified to light brown. The solution was cooled and dried at room temperature. The solid product was resumed with acetone, filtered off, washed with acetone and air-dried. Analysis found: Ca, 5.87; Cu, 4.59; C, 50.01; H, 6.64; N, 2.02, $Ca_2CuC_{56}H_{90}N_2O_{17}Cl_4$ calculate: Ca, 5.94; Cu, 4.71; C, 49.87; H, 6.73; N, 2.07 %; Yield 67 %; ESI–MS (positive mode, DMF:CH_3OH) *m/z*: $[M\text{-}5H_2O\text{–}2CH_3 + 5H]^+$, 1233.6; $[CaCuC_{54}H_{80}N_2O_{12}Cl_3]^+$, 1159.7; $[CaCuC_{53}H_{77}N_2O_{12}Cl_3]^+$, 1144.6; $[CaCuC_{54}H_{80}N_2O_{12}Cl_3]^+$, 1108.5; $[CuC_{55}H_{73}N_2O_{12}]^+$, 1017.7; $[CuC_{54}H_{73}N_2O_{12}]^+$, 1005.5; $[CuC_{53}H_{70}N_2O_{12}]^+$, 990.5; $[CuC_{47}H_{60}N_2O_{12}]^+$, 908.4; $[CuC_{53}H_{70}N_2O_{12}]^+$, 990.5; $[Ca_2CuC_{30}H_{40}N_2O_{10}Cl_4]^+$, 872.4; $[Ca_2CuC_{32}H_{41}N_2O_{10}Cl_3]^+$, 863.9; $[Ca_2CuC_{31}H_{40}N_2O_{10}Cl_3]^+$, 850.5; $[Ca_2CuC_{29}H_{30}N_2O_{10}Cl_3]^+$, 816.8; $[CuC_{40}H_{55}N_2O_6]^+$, 723.3; $[CuC_{39}H_{53}N_2O_6]^+$, 709.3; $[CaC_{28}H_{37}NO_6Cl_2]^+$, 594.7; $[CaC_{27}H_{36}NO_6Cl_2]^+$, 581.7; $[CaC_{28}H_{41}NO_6Cl]^+$, 563.5; $[C_{28}H_{38}NO_6]^+$, 484.2; $[C_{27}H_{34}NO_6]^+$, 468.4; $[C_{25}H_{32}NO_6]^+$, 442.1; $[C_{24}H_{30}NO_6]^+$, 428.1; $[C_{18}H_{34}NO_5]^+$, 344.3; $[C_{15}H_{27}NO_5]^+$, 301.4; $[C_{15}H_{28}NO]^+$, 226.3; $[C_{11}H_{16}O]^+$, 164.0; $[C_7H_8N]^+$, 106.6; $[C_6H_{11}]^+$, 83.4; $[C_6H_{11}]^+$, 83.4; Λ_M, 319 Ω^{-1} cm^2 mol^{-1}.

Results and discussion

Synthesis and physico-chemical characterisation of complexes

The crowned Schiff bases are of interest since they can bind both alkali and transition metals, and thus the property of each metallic ion can be influenced by the other. Such a species having two donor atom sets was synthesised by 1:1 condensation of 2-hydroxy-8-methyl-tricyclo[7,3,1,02,7]-13-one-tridecane with 4′-aminobenzo-15-crown-5-ether.

The reaction of this ligand with copper(II) chloride in the 2:1 molar ratio, with calcium(II) chloride in 1:1 molar ratio and with both salts in 2:1:2 molar ratio yields three new complexes as presented in Scheme 1. The compounds were formulated as $[Ca(HL)(OH_2)_4]Cl_2{\cdot}4H_2O$

(**1**), $[CuL_2]\cdot 2H_2O$ (**2**) and $[Cu\{Ca(L)(OH_2)_2\}_2]Cl_4\cdot H_2O$ (**3**) on the basis of elemental analyses (experimental part) and physico-chemical data presented below. The molar conductivities in DMF indicate the non-electrolyte nature of complex (**2**), while complex (**1**) behaves as 1:2 electrolyte and complex (**4**) as 1:4 electrolyte [33]. All complexes are soluble in water and the common organic solvents.

ESI MS and NMR spectra

The pseudomolecular ion peaks as well as that corresponding to some fragments either of ligand or of complexes fragmentation support the proposed structure for the basic core. As expected, the spectrum of complex (**3**) is the most complex. In the mass spectra of all complexes, the pseudomolecular ion peaks were detected as $[M\text{-}4H_2O\text{–}3H]^+$ (*m/z* 594.7) for (**1**), $[M\text{-}H_2O\text{–}CH_3\text{–}4H]^+$ (*m/z* 1017.7) for (**2**) and $[M\text{-}5H_2O\text{–}2CH_3 + 5H]^+$ (*m/z* 1233.6) for (**3**), respectively. The pseudomolecular ion peak $[M\text{-}3H]^+$ for the free Schiff base was detected at *m/z* 484.2. Moreover, other fragments corresponding either to crown ether moiety or to tricyclo part were identified in the spectra of all complexes and Schiff base.

The ^1H NMR and ^{13}C NMR spectral data for Schiff base and diamagnetic complex (**1**) are consistent with the Schiff base structure and exhibit as result signals corresponding to all functional groups. It is worth to mention that in the spectra of compounds (**1**) all signals are shifted as result of deuterated solvent changing but the most shifted both downfield and upfield are that assigned to crown ether moiety.

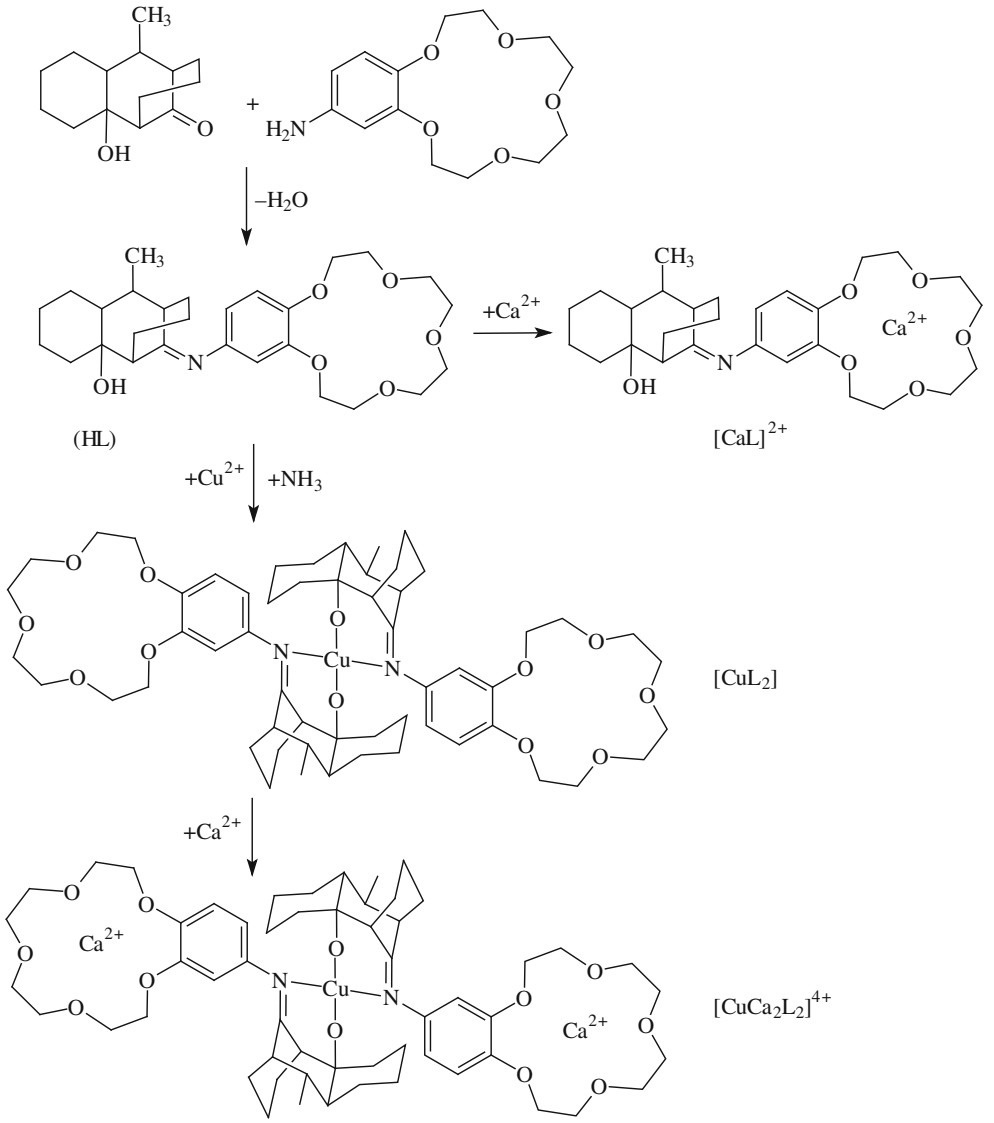

Scheme 1 Synthetic route to prepare ligand and complexes (water molecules were omitted)

Infrared spectra

The IR selected bands of the Schiff base and complexes are listed in Table 1. The stretching mode of the azomethine moiety ν(C=N) appears at 1610 cm^{-1} in the spectrum of Schiff base and is readily assigned by comparison with the infrared spectra of intermediates, 2-hydroxy-8-methyl-tricyclo[7,3,1,02,7]-13-one-tridecane and 4′-aminobenzo-15-crown-5-ether, respectively. The spectra of all complexes display also a very strong band around 1600 cm^{-1} (Fig. 2S). This band is shifted to higher wavenumbers for complex (**1**) and lower wavenumbers for complexes (**2**) and (**3**) in comparison with the free ligand. Such a shift supports the participation of the azomethine nitrogen in coordination for complexes (**2**) and (**3**) [34, 35].

The stretching vibration ν(C–O) of the hydroxyl group is shifted to lower wavenumbers in the complexes (**2**) and (**3**) spectra suggesting the participation of this deprotonated group in coordination [36]. Moreover, the strong band at 3395 cm^{-1} in the Schiff base spectrum disappears in complexes spectra as result of hydroxyl group deprotonation. Instead, a broad band in the range 3410–3490 cm^{-1} that appears in the spectra of complexes can be assigned to ν(OH) stretching vibration of water molecules [37], presence confirmed by elemental and thermal analyses as well.

The absorptions found at values characteristic for aromatic and aliphatic ether groups of crown ether moiety [4] are shifted to lower values in the spectra of complexes (**1**) and (**3**) as result of interaction with calcium ion [38].

Table 1 Absorption maxima (cm^{-1}) from IR spectra and assignments for the Schiff base and complexes (**1**)–(**3**)

HL	(**1**)	(**2**)	(**3**)	Assignment
–	3490s	3433m	3410s	$\nu(OH_2)$
3395s	3390vs	–	–	ν(OH)
2921m	2939vs	2922m	2937s	$\nu_{as}(CH_2)$
2862m	2858m	2869m	2875m	$\nu_s(CH_2)$
–	1708s	–	1707m	$\delta(OH_2)$
1610m	1634m	1593m	1601m	ν(C=N)
1511vs	1516m	1508vs	1507s	$\delta(CH_2)$
1453m	1444m	1451m	1453s	ν(C=C)
1249m	1217m	1254m	1227m	ν_{as}(Ar–O–C)
1181m	1177m	1156m	1152m	ν(C–O)
1128vs	1097m	1128s	1087m	ν(C–O–C)
1061m	1051m	1060m	1057m	ν_{sym}(Ar–O–C)
897m	903w	851w	853w	γ(CH)aromatic
846m	840w			
–	551w	525w	581w	ν(M–O)
			550w	
–	–	460w	460w	ν(M–N)

vs very strong, *s* strong, *m* medium, *w* weak

Electronic, EPR spectra and magnetic moments

Electronic spectra correlated with magnetic moments at room temperature provide useful information concerning both oxidation state of copper ion and stereochemistry. Table 2 lists the electronic absorption bands and magnetic moments of complexes in solid state.

The intraligand $n\rightarrow\pi^*$ and $\pi\rightarrow\pi^*$ transitions resulted from the –C=C– (aromatic ring) and –C=N– groups are different shifted in the complexes spectra as result of changes in the electronic density of the ligand upon coordination.

The electronic spectra of complexes (**2**) and (**3**) show a broad band at 16,950/16,530 cm^{-1} assigned to $d_{z^2} \rightarrow d_{x^2-y^2}$ transition in a rhombic distorted stereochemistry [39]. Such stereochemistry can be a square planar one with different donor atoms arranged in the *trans* disposition. The values of the magnetic moment for Cu(II) complexes are typical for Cu(II) compounds without interaction between paramagnetic ions [40].

The powder EPR spectra for complexes (**2**) and (**3**) recorded at room temperature exhibit a broad and asymmetric band with the part at lower field broader than at higher field (Fig. 1). The peak-to-peak line width is 242 G for the complex (**2**) and 223 G for the complex (**3**) while the g values are very close, 2.1272 for complex (**2**) and 2.1195 for complex (**3**), respectively. The similar features of the EPR spectra can be related to a square planar stereochemistry with grossly misaligned tetragonal axes [41].

Table 2 Absorption maxima (cm^{-1}) from electronic spectra of ligand and complexes (**1**)–(**4**), assignments and magnetic moments

Compound	Absorption maxima/cm^{-1}	Assignments	Magnetic moment/B.M.
HL	40,815	$n\rightarrow\pi^*$	–
	33,330		
	25,315	$\pi\rightarrow\pi^*$	
	17,540		
$[Ca(HL)(OH_2)_4]Cl_2{\cdot}4H_2O$ (**1**)	40,815	$n\rightarrow\pi^*$	–
	33,900		
	17,860	$\pi\rightarrow\pi^*$	
$[CuL_2]{\cdot}2H_2O$ (**2**)	40,000	$n\rightarrow\pi^*$	1.87
	37,040		
	24,690	$\pi\rightarrow\pi^*$	
	16,950	$d_{z^2} \rightarrow d_{x^2-y^2}$	
$[Cu\{Ca(L)(OH_2)_2\}_2]Cl_4{\cdot}H_2O$ (**3**)	40,810	$n\rightarrow\pi^*$	1.80
	37,040		
	27,780	$\pi\rightarrow\pi^*$	
	18,350		
	16,530	$d_{z^2} \rightarrow d_{x^2-y^2}$	

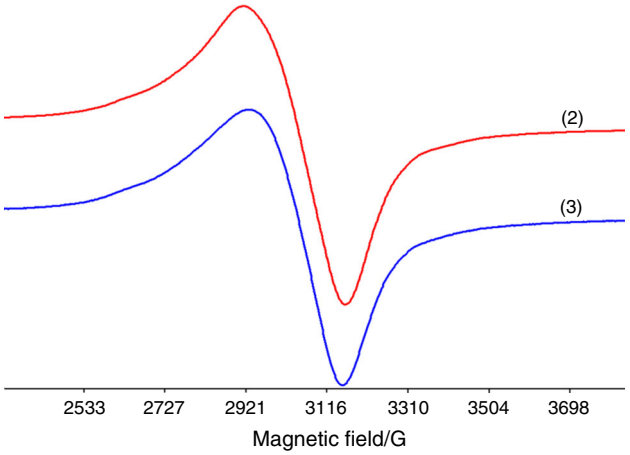

Fig. 1 X-band powder EPR spectra for complexes (**2**) and (**3**)

Thermal behaviour of complexes

The thermal analysis is frequently used in order to get useful information concerning the composition and stability of complexes. As result, the thermal behaviour of ligand and complexes was investigated in air by simultaneous TG/DTA analysis, while the final residue was examined by powder X-ray diffraction and IR spectroscopy, respectively.

The thermal decomposition data are summarised in Table 3 and will be discussed as follows.

Thermal decomposition of Schiff base

The TG, DTG and DTA curves registered for crowned Schiff base are shown in Fig. 2 and indicate that the compound is stable up to 215 °C and then undergoes two steps thermal decomposition. The small exothermic peaks observed on DTA curve in the 215–434 °C temperature range are probably due to both endothermic and exothermic reactions that occur simultaneously, such as cleavage and rearrangement of the covalent bonds as well as some moieties oxidative degradation. According to the mass loss, about 65 % of the Schiff base is eliminated through these processes up to 434 °C, loss that correspond to oxidative degradation of benzocrown moiety together with C=N unit and methyl group (found/calc.: 64.0/63.2 %). In the final step, the rest of organic part oxidative degradation occurs, accompanied by several strong overlapped exothermic processes as can be noticed on DTA curve (found/calc.: 36.0/36.8 %).

Thermal decomposition of $[Ca(HL)(OH_2)_4]Cl_2{\cdot}4H_2O$ (1)

The TG, DTG and DTA curves corresponding to the complex (**1**) indicate that decomposition follows five well-defined steps (Fig. 3). Chemical analysis indicate the presence of eight water molecule per metallic ion while the thermal

Table 3 Thermal behaviour data (in synthetic air atmosphere) for complexes

Compound	Step	Thermal effect	Temperature range/°C	Δm_{exp}/%	Δm_{calc}/%	Process
HL	1.	Exothermic	215–434	64.0	63.2	Oxidative degradation of benzocrown, imine and methyl moieties
	2.	Exothermic	434–655	36.0	36.8	Oxidative degradation of the rest of Schiff base
$[Ca(HL)(OH_2)_4]{\cdot}4H_2O$ (**1**)	1.	Endothermic	64–150	10.1	9.7	Water elimination
	2.	Endothermic	150–193	10.0	9.7	Water elimination
	3.	Exothermic	193–274	12.7	12.9	Oxidative degradation of cyclohexyl alcohol moiety
	4.	Exothermic	274–350	17.1	16.5	Oxidative degradation of ethylcyclohexyl imine moiety
	5.	Exothermic	355–705	35.1	36.3	Oxidative degradation of the rest of Schiff base
	Residue: $CaCl_2$			15.0	14.9	
$[CuL_2]{\cdot}2H_2O$ (**2**)	1.	Endothermic	124–168	3.4	3.4	Water elimination
	2.	Exothermic	168–472	49.8	49.8	Oxidative degradation of benzocrown moiety
	3.	Exothermic	400–715	39.2	39.3	Oxidative degradation of the rest of Schiff base
	Residue: CuO			7.6	7.5	
$[Cu\{Ca(L)(OH_2)_2\}_2]Cl_4{\cdot}H_2O$ (**3**)	1.	Endothermic	60–90	1.2	1.3	Water elimination
	2.	Endothermic	140–223	5.1	5.3	Water elimination
	3.	Exothermic	210–428	30.5	30.4	Oxidative degradation of tricycle moiety
	4.	Exothermic	428–735	34.8	34.8	Oxidative degradation of the rest of Schiff base
	5.	Exothermic	735–900	5.8	5.8	Residual carbon burning
	Residue: $CuO + CaCl_2$			22.6	22.4	

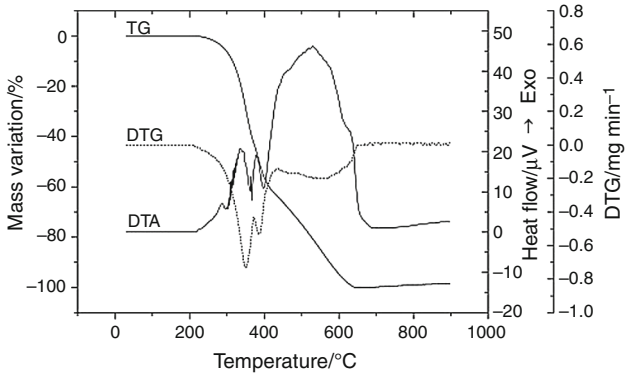

Fig. 2 TG, DTG and DTA curves for HL

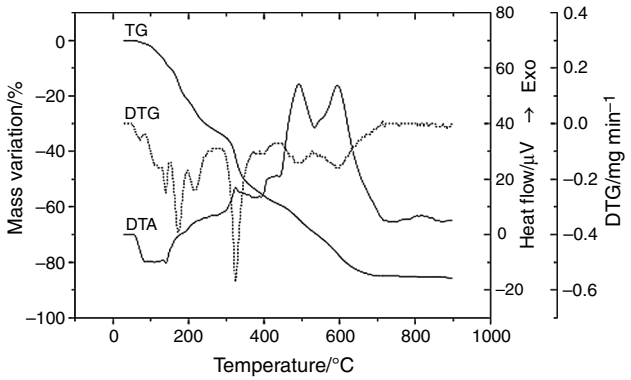

Fig. 3 TG, DTG and DTA curves for $[Ca(HL)(OH_2)_4]\cdot 4H_2O$ (**1**)

behaviour indicates that these molecules are involved in different interactions considering that they are eliminated in two well-defined steps. First, four water molecules are eliminated up to 150 °C (found/calc.: 10.1/9.7 %) while the remaining four are eliminate up to 193 °C (found/calc.: 10.0/9.7 %), both processes being accompanied by an endothermic effect. The temperature ranges corresponding to these steps indicate the role of this species both as crystallisation [42] and as coordination [43, 44], both types being involved in additional strong hydrogen bonds.

According to mass loss, in the third step the cyclohexyl alcohol unit of Schiff base elimination occurs in several weak exothermic, overlapped processes (found/calc.: 12.7/12.9 %). This feature of the DTA curve could arise again from cleavage of the covalent bonds, their rearrangement and some moieties oxidative degradation, processes accompanied by both endothermic and exothermic effects. The oxidative degradation of ethylcyclohexyl imine moiety occurs in the next step, being accompanied by an exothermic effect (found/calc.: 17.1/16.5 %). In the last step occurs the oxidative degradation of the remaining part of Schiff (found/calc.: 35.1/36.3 %), step that is not a single one but an overlap of at least three processes according to both DTG and DTA curves profile. According to overall mass loss, the final residue is $CaCl_2$ (found/calc.: 85.0/85.1 %). The residue is amorphous since no signal was observed in powder XRD spectrum, and as result its nature as $CaCl_2$ was assigned by the appearance of a band at 520 cm^{-1} in the IR spectrum that can be assigned to ν(Ca–Cl) vibration mode.

Thermal decomposition of $[CuL_2]\cdot 2H_2O$ (2)

Complex (**2**) losses the crystallisation water up to 168 °C (found/calc.: 3.4/3.4 %), temperature that is higher as result of the fact that water is trapped insight of the crown ether moiety through strong hydrogen bonds. Otherwise, such an interaction was observed for other crown ether derivatives [45].

The oxidative degradation of the Schiff base begins with benzocrown group elimination (found/calc.: 49.8/49.8 %), process accompanied by several weak endothermic effects (Fig. 4). The mass loss up to 715 °C corresponds to oxidative degradation of the remaining part of the Schiff base (found/calc.: 39.2/39.3 %), and according to DTA curve, several overlapped processes occur until the CuO is formed (PDF 80-1916) (found/calc. overall mass loss: 92.4/92.5 %).

Thermal decomposition of $[Cu\{Ca(L)(OH_2)_2\}_2]Cl_4\cdot H_2O$ (3)

For complex (**3**), the water molecules are also stepwise eliminated, namely the crystallisation one up to 90 °C (found/calc.: 1.2/1.3 %) [42], while the coordination one in 140–223 °C temperature range (found/calc.: 5.1/5.3 %) [43, 44]. As it can see in Fig. 5, both steps are endothermic. The first step occurs up to a lower temperature comparing with compound (**2**). The explanation could be the involvement of water molecules in weak hydrogen interactions having in view that the cavity of the crown ether is occupied by the Ca(II) ion. The diminishing of the hydrogen bonds interaction with decreasing the water

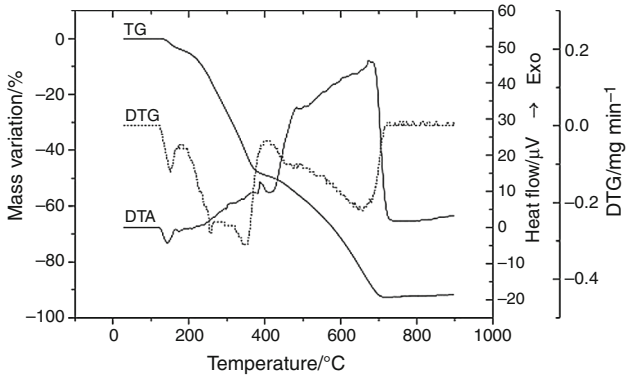

Fig. 4 TG, DTG and DTA curves for $[CuL_2]\cdot H_2O$ (**2**)

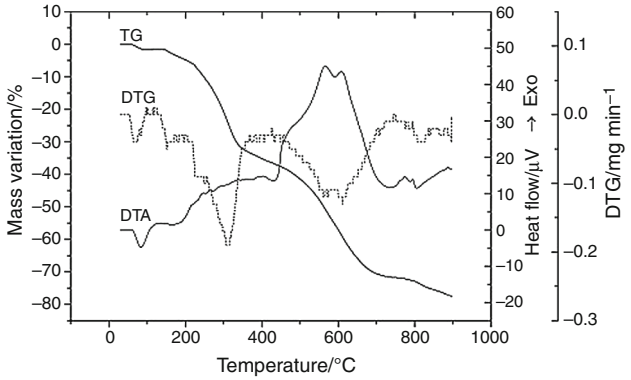

Fig. 5 TG, DTG and DTA curves for $[Cu\{Ca(L)(OH_2)_2\}_2]Cl_4{\cdot}H_2O$ (**3**)

molecule number was also observed for other Ca(II) complexes [46].

The oxidative degradation starts with tricycle moiety (found/calc.: 30.5/30.4 %), and several weak exothermic effects can be observed on DTA curve as result of superposition of several processes, accompanied by both endothermic and exothermic effects. The oxidative degradation of the remaining part of Schiff occurs in the next step (found/calc.: 34.8/34.8 %), accompanied by a strong exothermic effect. This step is not a single one but an overlap of three processes according to both DTG and DTA curves profile. A small quantity of residual carbon remains trapped in the lattice (found/calc.: 5.8/5.8 %) and burns in the last step with a mixture of $CaCl_2$ and CuO generation (PDF 80-1916) (found/calc. overall mass loss: 77.4/77.6 %). In the IR spectrum of residue, the band at 470 cm^{-1} was assigned to ν(Cu–O) vibration mode while that at 517 and 579 cm^{-1} arise from ν(Ca–Cl) vibration modes.

Antioxidant activity

The antioxidant activity reflects the ability of a certain compound to inhibit the generation of reactive oxygen species (ROS) and all accompanied processes that end with the cell destruction [29]. The dpph method indicates that the obtained compounds exhibit a weak antioxidant activity (Table 4), except for compound (**3**) with a TAC value of 93 %.

Antimicrobial activity

The qualitative screening of the antimicrobial activity of the tested compounds performed on gram-negative and gram-positive bacteria, as well as fungal strains revealed that the compound (**3**) proved to be more active than ligand against *S. aureus, B. subtilis* and *E. coli,* followed by compound (**2**) which was slightly more active than ligand against *E. coli*.

Table 4 Total antioxidant activity (TAC) of compounds

Compound	TAC/%
HL	46.33
(**1**)	24.07
(**2**)	18.49
(**3**)	93.80

The results of the quantitative assay of the antimicrobial activity of the tested compounds against the microbial strains in planktonic growth state revealed that all three complexes exhibited in some cases an antimicrobial activity superior to that of the ligand, namely compound (**1**) against *S. aureus* and *C. albicans* and compound (**3**) against *C. albicans* (Table 5). However, both the ligand and the derived compounds exhibited very low MIC values ranging from 7.8 to 62.5 μg mL^{-1} against the majority of the tested strains.

The assay of the minimal biofilm eradication concentration reflecting the inhibitory activity of the tested compounds against the microbial strains in sessile growth state revealed a decreased efficiency of the tested compounds against the adhered cells as demonstrated by the higher MBEC as compared to MIC values (Table 6). However, compound (**1**) exhibited a superior antibiofilm activity as compared to that of the ligand against *S. aureus* and *B. sutbtilis* and compound (**3**) against *E. coli* and *C. albicans*. However, it is to be noticed that both the ligand and the derived compounds proved to be very active against *P. aeruginosa* biofilm, exhibiting a MBEC value of 62.5 μg mL^{-1}. It is also to be noticed the high antibiofilm efficiency of compound (**1**) against *S. aureus* biofilms. Taking into account the high prevalence of these two

Table 5 MIC (μg mL^{-1}) values of the tested compounds against the tested microbial strains

Strain	HL	(**1**)	(**2**)	(**3**)
S. aureus	31.2	7.8	125	62.5
B. subtilis	31.2	31.2	62.5	31.2
P. aeruginosa	62.5	62.5	62.5	62.5
C. albicans	125	62.5	–	62.5

Table 6 MBEC (μg mL^{-1}) values of the tested compounds against the tested microbial strains

Strain	HL	(**1**)	(**2**)	(**3**)
S. aureus	62.5	31.2	62.5	62.5
B. subtilis	62.5	31.2	125	125
E. coli	0.25	250	1000	62.5
P. aeruginosa	62.5	125	125	62.5
C. albicans	62.5	62.5	1000	31.2

Table 7 Flow cytometry quantification of HCT 8 cell viability in the presence of ligand and complexes assayed by Annexin-FITC/PI Kit

Cell viability	HCT 8	HL	(**1**)	(**2**)	(**3**)
Necrotic cells	2.35	1.21	1.33	2.17	1.84
Late apoptosis	1.14	1.25	2.87	5.61	7.54
Early apoptosis	0.26	3.74	6.41	1.96	3.16
Viable cells	96.2	93.8	89.4	90.3	87.5

bacterial species in the aetiology of chronic and biofilm-associated infections, which are very resistant to current antimicrobial regimens, the obtained results highlight the potential of these complexes for the development of novel antimicrobial and antibiofilm strategies.

Cytotoxic activity

In order to establish the treatment effect and to discriminate between intact and apoptotic HCT 8 cells, Annexin V-FITC Apoptosis Detection Kit I was used. All complexes exhibited an acceptable, low level of cytotoxicity. However, it could be stated that compound (**3**) was the most toxic (87.5 % viability), followed by (**1**) (89.4 % viability) (Table 7).

Conclusions

New complexes $[Ca(HL)(OH_2)_4]Cl_2{\cdot}4H_2O$ (**1**), $[CuL_2]{\cdot}2H_2O$ (**2**) and $[Cu\{Ca(L)(OH_2)_2\}_2]Cl_4{\cdot}H_2O$ (**3**) were synthesised and characterised by reaction of metal chloride with Schiff base 2-hydroxy-8-methyl-tricyclo[7.3.1.$0^{2.7}$]-tridec-13-N-4′(benzo-15-crown-5-ether)-imine (HL) in alkaline medium.

IR spectra display the characteristic features of the crowned Schiff bases and indicate that ligand acts as bis-chelate through azomethinic nitrogen and phenolic oxygen in interaction with Cu(II) ion and trapped Ca(II) in crown ether moiety. Complexes display square planar stereochemistry in concordance with UV–Vis and EPR spectra patterns.

Thermal decomposition of complexes allowed establishing the number and nature of water molecule, the composition of complexes and also the intervals of thermal stability. After water elimination in one or two well-defined events, the complexes suffer oxidative degradation of Schiff base leading to the most stable species as final product.

The results of the biological assays revealed that tested compounds exhibited good antimicrobial activity against planktonic bacterial and fungal strains, as revealed by the very low MIC values. In case of compounds (**1**) and (**3**), the antimicrobial activity was improved compared to that of ligand against *S. aureus* and *C. albicans*. Compounds exhibited also antibiofilm activity, but the MBEC values were generally higher than the MIC ones. The compounds (**1**) and (**3**) exhibited a superior antibiofilm activity compared to that of ligand against *S. aureus, B. sutbtilis, E. coli* and *C. albicans*. Taking into account the results of antimicrobial assay correlated with the low cytotoxicity against human cells, it could be stated that the obtained complexes could be promising for the further development of novel antimicrobial and antibiofilm agents.

Acknowledgements The authors thank to Nicolae Stanică from "Ilie Murgulescu" Physical Chemistry Institute, Romanian Academy for the help with magnetic measurements at room temperature and Romana Cerc Korosec from University of Ljubljana, Faculty of Chemistry and Chemical Technology, Department of Inorganic Chemistry, Ljubljana, Slovenia for powder XRD measurements.

References

1. Vigato PA, Tamburini S. Advances in acyclic compartmental ligands and related complexes. Coord Chem Rev. 2008;252:1871–995.
2. Dubonosov AD, Minkin VI, Bren VA, Shepelenko EN, Tsukanov AV, Starikov AG, Borodkin GS. Tautomeric crown-containing chemosensors for alkali-earth metal cations. Tetrahedron. 2008;64:3160–7.
3. Şahin D, Koçoğlu S, Şener O, Şenol C, Dal H, Hökelek T, Hayvalı Z. New NO donor ligands and complexes containing furfuryl or crown ether moiety: syntheses, crystal structures and tautomerism in ortho-hydroxy substituted compounds as studied by UV–Vis spectrophotometry. J Mol Struct. 2015;1102:302–13.
4. Pedras B, Fernandes L, Oliveira E, Rodríguez L, Raposo MMM, Capelo JL, Lodeiro C. Synthesis, characterization and spectroscopic studies of two new Schiff-base bithienyl pendant-armed 15-crown-5 molecular probes. Inorg Chem Commun. 2009;12:79–85.
5. Sousa C, Freire C, de Castro B. Synthesis and characterization of benzo-15-crown-5 ethers with appended N_2O Schiff bases. Molecules. 2003;8:894–900.
6. Sahin D, Hayvali Z. Syntheses, spectroscopic characterization and metal ion binding properties of benzo-15-crown-5 derivatives and their sodium and nickel(II) complexes. J Incl Phenom Macrocycl Chem. 2012;72:289–97.
7. Shimakoshia H, Maedaa D, Hisaeda Y. Supramolecular assemblies of crown-substituted dinickel and dicobalt complexes with guest cation binding. Supramol Chem. 2011;23:131–9.
8. Beer PD, Gale PA, Chen GZ. Mechanisms of electrochemical recognition of cations, anions and neutral guest species by redox-active receptor molecules. Coord Chem Rev. 1999;185–186:3–36.
9. Güler H, Hayvalı Z, Dal H, Hökelek T. Syntheses, spectroscopic and structural characterizations and metal ion binding properties of Schiff bases derived from 4′-aminobenzo-15-crown-5. Polyhedron. 2012;31:688–96.
10. Hayvalı Z, Köksal P. Syntheses and spectroscopic characterization of double-armed benzo-15-crown-5 derivatives and their sodium and potassium complexes. J Incl Phenom Macrocycl Chem. 2013;76:369–78.
11. Hayvalı Z, Güler H, Öğütcü H, Sarı N. Novel bis-crown ethers and their sodium complexes as antimicrobial agent: synthesis and spectroscopic characterizations. Med Chem Res. 2014;23:3652–61.

12. Kryatova OP, Kolchinski AG, Rybak-Akimova EV. Metal-containing ditopic receptors for molecular recognition of diammonium cations. Tetrahedron. 2003;59:231–9.
13. Korybut-Daszkiewicz B, Bilewicz R, Wózniak K. Tetraimine macrocyclic transition metal complexes as building blocks for molecular devices. Coord Chem Rev. 2010;254:1637–60.
14. Sousa C, Gameiro P, Freire C, de Castro B. Nickel(II) and copper(II) Schiff base complexes bearing benzo-15-crown-5 functionalities as probes for spectroscopic recognition of lanthanide ions. Polyhedron. 2004;23:1401–8.
15. Martins M, Freire C, Hillman AR. Acoustic wave sensor for barium based on poly[Ni(*salen*)(crown)] recognition chemistry. Chem Commun. 2003;3:434–5.
16. Yi Y, Wang Y, Liu H. Preparation of new crosslinked chitosan with crown ether and their adsorption for silver ion for antibacterial activities. Carbohydr Polym. 2003;53:425–30.
17. Radwan AA, Alanazi FK, Alsarra IA. Microwave irradiation-assisted synthesis of a novel crown ether crosslinked chitosan as a chelating agent for heavy metal ions (M^{+n}). Molecules. 2010;15:6257–68.
18. Xie JQ, Chen Y, Li C, Zhu JJ, Hu W, Zeng XC. Hydrolysis of bis(4-nitrophenyl) phosphate catalyzed by metallomicelle made up of the crowned Schiff base complex as synthetic hydrolase. J Dispers Sci Technol. 2005;26:693–9.
19. Hu W, Wang Y, Yan J, Li JZ, Meng XG, Hu CW, Zeng XC. Hydrolysis of BNPP catalyzed by the crowned Schiff base Co(II) complexes in Micellar solution. J Dispers Sci Technol. 2006;27:1085–92.
20. Xu B, Jiang W, Zhang J, Tang Y, Li J. Effect of manganese(III) Schiff base complexes on the hydrolysis of *p*-nitrophenyl picolinate. Trans Met Chem. 2009;34:293–6.
21. Klein Gebbink RJM, Martens CF, Feiters MC, Karlin KD, Nolte RJM. Novel molecular receptors capable of forming Cu_2–O_2 complexes. Effect of preorganization on O_2 binding. Chem Commun. 1997;4:389–90.
22. Zeng W, Li J, Qin S. The effect of aza crown ring bearing salicylaldimine Schiff bases Mn(III) complexes as catalysts in the presence of molecular oxygen on the catalytic oxidation of styrene. Inorg Chem Commun. 2006;9:10–2.
23. Sun B, Chen J, Hu J, Li X. Dioxygen affinities and catalytic oxidation activities of cobalt complexes with Schiff bases containing crown ether. J Inorg Biochem. 2006;100:1308–13.
24. Li J-Z, Wang Y, Zeng W, Qin S-Y. Synthesis and study of unsymmetrical schiff base Mn(III) complexes with pendant aza-crown or morpholino groups as catalyst in aerobic oxidation for p-xylene to p-toluic acid. Supramol Chem. 2008;20:249–54.
25. Li J-Z, Xu B, Jiang WD, Zhou B, Zeng W, Qin SY. Catalytic epoxidation performance and dioxygen affinities of unsymmetrical Schiff base transition–metal complexes with pendant aza-crown or morpholino groups. Trans Met Chem. 2008;33:975–9.
26. Seyedi SM, Zohuri GH, Sandaroos R. Synthesis and application of new Schiff base Mn(III) complexes containing crown ether rings as catalysts for oxidation of cyclohexene and cyclooctene by Oxone. Supramol Chem. 2011;23:509–17.
27. Wei H, Jian ZL, Ying W, Ju D, Chang WH, Xian CZ. Studies on phenol oxidation with H_2O_2 catalyzed by Schiff base cobalt(II) complexes in Micellar solution. J Dispers Sci Technol. 2008;29:1476–83.
28. Bassett J, Denney RC, Jeffery GH, Mendham J. Vogel's textbook of quantitative inorganic analysis (Fourth edition). New York: The English Language Book Society and Logman; 1978.
29. Belkheiri N, Bouguerne B, Bedos-Belval F, Duran H, Bernis C, Salvayre R, Negre-Salvayre A, Baltas M. Synthesis and antioxidant activity evaluation of a syringic hydrazones family. Eur J Med Chem. 2010;45:3019–26.
30. Calu L, Badea M, Chifiriuc MC, Bleotu C, David G-I, Ioniţă C, Măruţescu L, Lazăr V, Stanică N, Irina Soponaru I, Dana Marinescu D, Olar R. Synthesis, spectral, thermal, magnetic and biological characterization of Co(II), Ni(II), Cu(II) and Zn(II) complexes with a Schiff base bearing a 1,2,4-triazole pharmacophore. J Therm Anal Calorim. 2015;120:375–86.
31. Barbulescu N. Condensarea ciclohexanonei cu aldehide. Rev Chem (Bucharest). 1956;7:45–52.
32. Coic J-P, Rollin P, Setton R. Condensation de la cyclohexanone par les alcoolates alcalins en solution. C R Acad Sci Paris. 1969;t268:1964–6.
33. Geary WJ. The use of conductivity measurements in organic solvents for the characterisation of coordination compounds. Coord Chem Rev. 1971;7:81–122.
34. Zayed EM, Zayed MA, Hindy AMM. Thermal and spectroscopic investigation of novel Schiff base, its metal complexes, and their biological activities. J Therm Anal Calorim. 2014;116:391–400.
35. Khalaji AD, Nikookar M, Das D. Co(III), Ni(II), and Cu(II) complexes of bidentate N, O-donor Schiff base ligand derived from 4-methoxy-2-nitroaniline and salicylaldehyde Synthesis, characterization, thermal studies and use as new precursors for metal oxides nanoparticles. J Therm Anal Calorim. 2014;115:409–17.
36. Rathore K, Singh RKR, Singh HB. Structural, spectroscopic and biological aspects of O, N-donor Schiff base ligand and its Cr(III), Co(II), Ni(II) and Cu(II) complexes synthesized through green chemical approach. E-J Chem. 2010;7:566–72.
37. Nakamoto K. Infrared and Raman spectra of inorganic and coordination compounds. 6th ed. In: Part B. Applications in coordination, organometallic, and bioinorganic chemistry. New Jersey: Wiley; 2009.
38. Guler H, Hayval Z, Dal H, Hokelek T. Syntheses, spectroscopic and structural characterizations and metal ion binding properties of Schiff bases derived from 4′-aminobenzo-15-crown-5. Polyhedron. 2012;31:688–96.
39. Solomon EI, Lever ABP (editors). Inorganic electronic structure and spectroscopy, Vol. II. In: Applications and case studies. New York: Wiley; 2006.
40. Gispert JR. Coordination chemistry. Weinheim: Wiley-VCH; 2008.
41. Kokoszka GF, Duerst RW. EPR studies of exchange coupled metal ions. Coord Chem Rev. 1970;5:209–44.
42. Dametto PR, Ambrozini B, Caires FJ, Franzini VP, Ionashiro M. Synthesis, characterization and thermal behaviour of solid-state compounds of folates with some bivalent transition metals ions. J Therm Anal Calorim. 2014;115:161–6.
43. El Metwally NM, Arafa R, El-Ayaan U. Molecular modeling, spectral, and biological studies of 4-formylpyridine-4N-(2-pyridyl) thiosemicarbazone (HFPTS) and its Mn(II), Fe(III), Co(II), Ni(II), Cu(II), Cd(II), Hg(II), and UO_2(II) complexes. J Therm Anal Calorim. 2014;115:2357–67.
44. Abdel-Kader NS, Amin RM, El-Ansary AL. Complexes of Schiff base of benzopyran-4-one derivative. Synthesis, characterization, non-isothermal decomposition kinetics and cytotoxicity studies. J Therm Anal Calorim. 2016;123:1695–706.
45. Minacheva LKh, Aleksandrov GG, Lapkina LA, Gorbunova YuG, Demin SV, Larchenko VE, Sergienko VS, Tsivadze AYu. Rosenmund–Braun reaction products 4′,5′-dicyanobenzo-15-crown-5 and 4′,5′-dicyanobenzo-15-crown-5,4′-cyano-5′-cyano(-bromo)benzo-15-crown-5 hydrates: spectroscopic properties and crystal structure. Russ J Coord Chem. 2005;31:671–82.
46. Hundal G, Hundal MS, Obrai S, Poonia NS, Kumar S. Metal complexes of tetrapodal ligands: synthesis, spectroscopic and thermal studies, and X-ray crystal structure studies of Na(I), Ca(II), Sr(II), and Ba(II) complexes of tetrapodal ligands N, N, N', N'-tetrakis(2-hydroxypropyl)ethylenediamine and N, N, N', N'-tetrakis(2-hydroxyethyl)ethylenediamine. Inorg Chem. 2002;41:2077–86.